Heat Transfer Mechanism In Particle-Laden Turbulent Shearless Flows

Société canadienne de

Society of Canada

Proceedings of the 30th Annual Conference of the Computational Fluid Dynamics Society of Canada

August 8-9, 2022

Table of Contents

Direct Numerical Simulation of Controlled Diffusion Airfoil Self-Noise Including Installation Effects

Andrea Arroyo Ramo, Stéphane Moreau, Richard D. Sandberg, Michaël Bauerheim, Marc C. Jacob

Direct Numerical Simulations (DNS) of the compressible flow passing over a Controlled Diffusion (CD) airfoil are conducted. A new 3D mesh topology based on overset meshes is used for the domain discretization as it provides flexibility when adapting the mesh to the boundary conditions (see changes in angle of attack). It is composed by two independent meshes, a background mesh and an o-grid structured overset mesh which can be oriented according to the required incidence angle.

The objective is to investigate the turbulent flow field close the airfoil surface (near field) at moderate Reynolds number focusing on the vicinity of the trailing edge, including the noise generation mechanisms near the trailing edge. Then, compute the acoustic far field using Amiet's classical trailing edge theory. The solver HiPSTAR, which uses a high-order finite-difference scheme in time and space, is used to compute the acoustic sources associated with self-noise on a real geometry of a turbomachinery component. The controlled diffusion airfoil is set at an incidence angle of 8º, embedded in a wind-tunnel flow a chord-based Reynolds number of 150000 and Mach number of 0.25. To represent experimental conditions, the installation effects are included by means of the boundary conditions of the simulation. Nonuniform inflow boundary conditions mimicking the anechoic open-jet facility characteristics are imposed. Such conditions are computed by 2D Reynolds Averaged Navier-Stokes (RANS) computations. Under these conditions, the flow on the suction side transitions from laminar to turbulent with the presence of a Laminar Separation Bubble near the leading edge. The pressure side remains fully attached up to the trailing edge where a vortex if found.

Three different spanwise discretization resolutions are computed and compared to evaluate its effect on the development of the turbulent structures. The aerodynamic field is compared to previous DNS calculations developed with HiPSTAR software with a mesh topology consisting in a body fitted domain composed by several refinement regions using interfaces. Satisfactory agreements with such previous DNS calculations as well as with experimental data from different wind tunnels set ups, mainly in the facilities of Université de Sherbrooke, TU-Delft and Ecole Centrale de Lyon ensure a proper reproduction of the experimental conditions. The acoustic far field predictions are satisfactory as well.

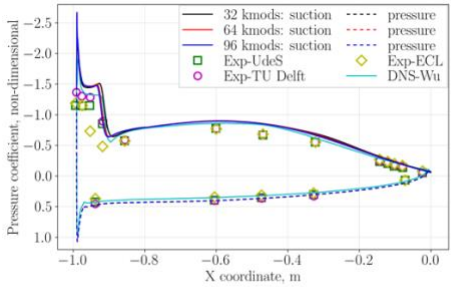

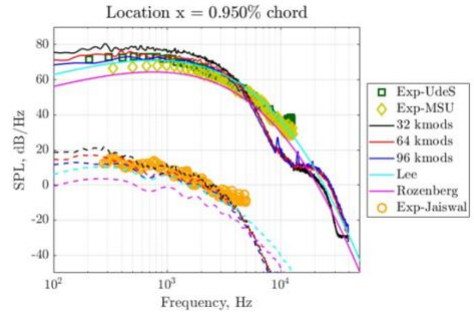

Numerical Investigation of a Pressure-Induced Laminar Separation Bubble on a Flat Plate

Augustin Cheret

With the alarming signals about climate change, many industrial sectors are improving their technologies to gain in efficiency. For turbomachine applications, from turbine for power generation to propeller or ventilation systems, computational fluid dynamics (CFD) is intensively used in design to optimize geometries and reduce losses associated to flow detachments. For investigating a large number of designs, classical Reynolds Averaged Navier-Stokes (RANS) approaches prevail based on rapid and robust predictions. Starting from a laminar Reynolds number of 10 based on the momentum thickness at the inlet, the present work will evaluate these approaches for the prediction of a transitioning boundary layer subjected to an adverse pressure gradient.

The investigated configuration reproduce the TFT boundary layer wind tunnel, specifically designed to study pressure-induced separation bubbles. Two-dimensional simulations on the 3 m long test-section are performed. The pressure gradient in the channel flow is controlled with a shaped wall and a slit on the opposite wall of the flat plate boundary layer under investigation. These critical features are carefully reproduced in the simulations. Both fully turbulent and transitional RANS simulations are performed with a reference inlet velocity of 4 m/s using the Shear Stress Transport model from F. Menter as implemented in ANSYS-CFX 2021R2.

The present work will evaluate the sensitivity of the boundary layer development to operating conditions, numerical parameters and turbulent modelling. Particular attention will be given to the inception of the transition, the boundary layer detachment and recirculation length, the reattachment and the rapid equilibrium return of the boundary layer. Several measurements available on the configuration will be used to identify the best reliable approaches under investigation.

Prediction of Turbulent Separation Over a Wall Mounted Hump with the Enhanced Detached Eddy Simulation Implemented in SU2

Ramin Taleban, François Morency, Marlène Sanjosé

The effects of ice accretion on airplane aerodynamics have drawn much attention in recent years. One of the challenges that engineers face is predicting the airplane's stall due to the complicated geometry of an iced aircraft wing. With the large flow separation caused by ice accretion, classical CFD simulations of the mean-field with the RANS models fail to predict aerodynamic forces. Given the Reynolds number of around 1 million, full unsteady and spatially resolved simulations are expensive (DNS/LES). Therefore, hybrid approaches such as Delayed Detached Eddy Simulations seem promising. Several experimental models are available to evaluate turbulence models and numerical approaches. The main objective is to validate the DDES method implemented in SU2 by looking at the Cp and Cf and the velocity profile. Within the NASACFDVAL2004 workshop, one of the documented test cases that has drawn much attention is the Wall Mounted Hump.

The test case can be interpreted as the separation on the upper surface of an airfoil over a hump representing ice accretion on the wing. For simulating this flow, an Enhanced DDES model with the Spalart Allmaras turbulence model base, as implemented in the SU2 solver is used in the present work. The space-numerical integration uses the scalar upwind method SLAU2 for the inviscid terms of the RANS equation. With the dual-timestep method for DDES, the convective and viscous fluxes are estimated at the middle edge of each cell. Accordingly, a Second-order MUSCL scheme with the Venkatakrishnan Wang limiter is used to stabilize the convective flux calculations. For the RANS solution, an Euler implicit scheme is used for time discretization. The computational domain of the WMH is the medium mesh (409x109) available on the NASA webpage, extended with 32 elements in the spanwise direction. The timestep is set in obedience to the grid spacing to ensure a CFL of around 1 is achieved at the area of interest. The initial part of the original domain is excluded to lower computation costs. With the EDDES-SA, the massive flow separation length is sensitive to turbulent transition that is triggered by the KH instability. The attached figure represents iso-surfaces of the instantaneous Q-Criterion downstream the hump at a random timestep. Cp, Cf and velocity will be analyzed and compared with the literature and experimental results. With improvements in hybrid approaches, CFD use will be more practical and could aid in predicting the icing effect.

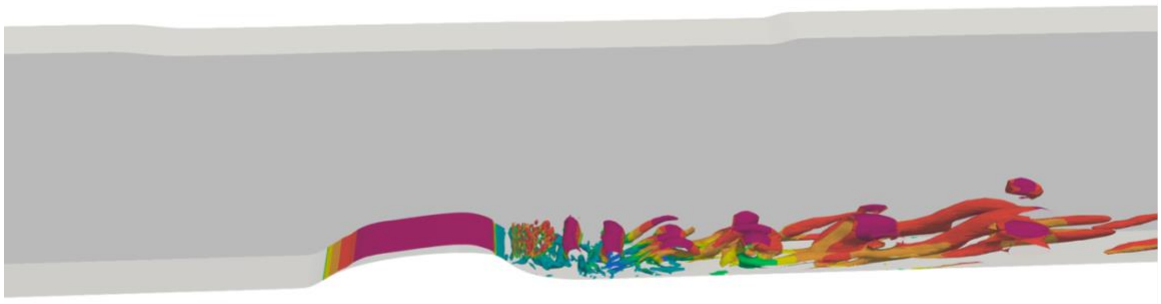

Large Eddy Simulation of a Linear Compressor Cascade with Tip Gap and End-Wall Motion: Aerodynamic and Acoustic analysis

Lorenzo Becherucci, Régis Koch, Stéphane Moreau

A wall-resolved compressible Large-Eddy Simulation has been performed on a linear compressor cascade with tip-gap and moving end-wall and is compared to a stationary endwall configuration in order to study its effects on the aerodynamics and the noise emission. The Ffowcs Williams and Hawkings acoustic analogy is used to compute the far-field noise and investigate the main noise sources related to the tip-clearance flow. This study provides the first wall-resolved compressible LES on a linear compressor cascade with a moving end-wall in order to investigate the noise related to the tip-leakage flow. The main aerodynamic structures such as the Tip-Leakage Vortex (TLV), the Tip Separation Vortex (TSV) and the Secondary Vorticity are resolved. The major effect of the sliding wall is seen in the flattening and entraining of the TLV from the blade SS towards the adjacent blade PS. Overall similar noise sources are found between the stationary and moving end-wall cases. Only the dipolar sound directivity is slightly shifted downstream with less marked lobes at high frequencies. Finally, a Dynamic Mode Decomposition performed on different planes inside of the passage has shown how the noise source caused by the tip separation vortex at 6 kHz is slightly moved upward at 50% chord instead of the 75% chord predicted in the stationary end-wall case.

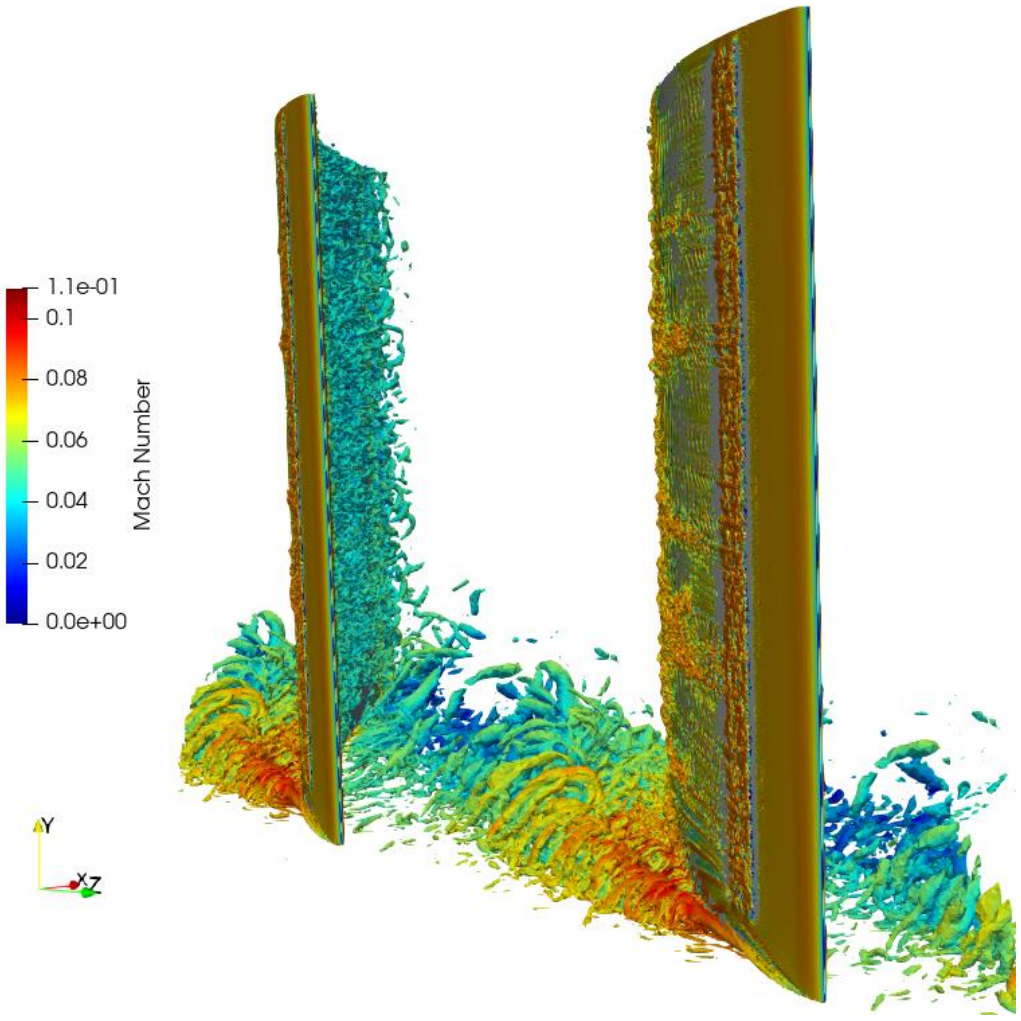

A New Generation of Explicit Runge-Kutta Schemes for Turbulent Flows

Brian C. Vermeire

The ability to perform accurate and efficient scale resolving simulations, such as Large Eddy Simulation (LES) and Direct Numerical Simulation (DNS), relies on suitable spatial and temporal discretization. Recent research has led to the development of a new generation of high-order unstructured methods, including the Discontinuous Galerkin (DG) and Flux Reconstruction (FR) approaches. These schemes are able to achieve arbitrarily high orders of accuracy, and explicit formulations are amenable to acceleration using Graphical Processing Units (GPUs). These properties make them well-suited for both LES and DNS. However, similar to other high-order methods, they suffer from relatively low maximum stable Courant Fredric's Lewy (CFL) numbers with explicit solvers. This means relatively small time steps must be taken, particularly for stiff problems such as high-Reynolds number flows with thin boundary layer elements.

In this talk we will introduce a new family of Paired Explicit Runge-Kutta (P-ERK) schemes. These schemes allow different explicit Runge-Kutta methods to be used in different parts of the domain, and can be optimized for any spatial discretization to yield that largest permissible time step size for a given number of Runge-Kutta stages. In this talk we will discuss the formulation of P-ERK schemes, their optimization for a FR/DG spatial discretizations, and performance and accuracy considerations. Then, we will introduce a new framework for embedded P-ERK schemes, which use a lower-order method to be used as an error/stability estimator, combined with a time-step size controller, to dynamically adapt the time step size based on evolving stability constraints.

The utility of embedded P-ERK schemes will then be demonstrated for a range of applications using the compressible Navier-Stokes equations including low Reynolds laminar flows, applications on moving and deforming domains, and unsteady turbulent flows using LES/DNS. These results demonstrate the P-ERK schemes consistently achieve speedup factors in excess of seven relative to classical explicit Runge-Kutta methods. This greatly extends the utility of high-order FR/DG schemes for applications to turbulent flows, greatly reducing their cost and increasing the industrial viability of a new generation of scales resolving CFD techniques.

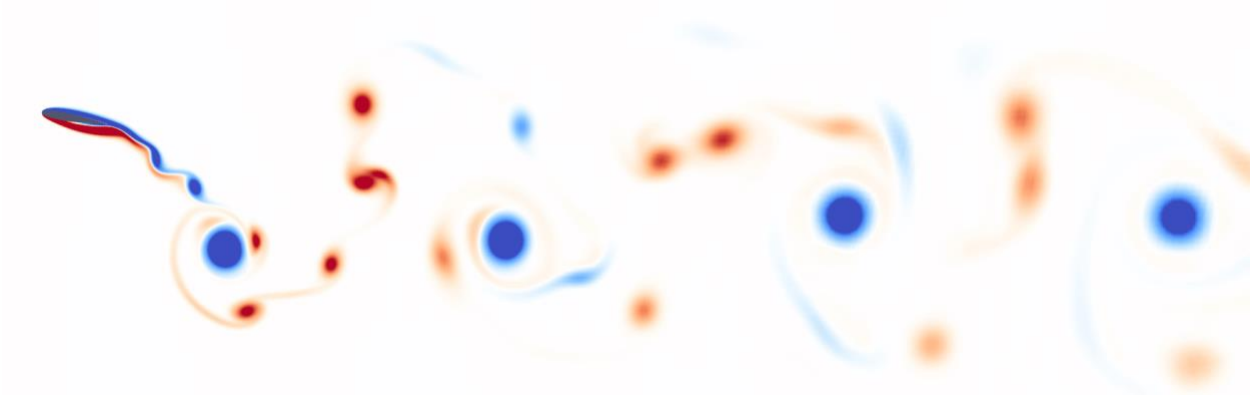

Role of Subgrid-Scale Turbulence in the Performance of Wind Farms

Jagdeep Singh, Jahrul Alam

Vertical kinetic energy entrainment by vortices at all length scales of atmospheric boundary layer flows can be a driving factor for the performance of large wind farms. In this article, we present a large eddy simulation of wind farms in neutral atmospheric boundary layers. Given the high Reynolds numbers and domain sizes on the order of kilometers, we cannot resolve the energy-containing vortices in the region, where the influence of Earth's surface reduces the size of vortices. Instead, we rely on vortex stretching and strain self-amplification to model the production of small-scale vortices by turbulence. We observe that the alignment between the vortex-stretching and the second invariant of the velocity gradient tensor can estimate the energy cascade rates from the resolved-scale motions to the subgrid-scale motions. In close proximity to the Earth's surface, we consider an ensemble of vortices attached to the surface and aligned in the streamwise direction. First, we have evaluated our LES method by comparing the results with the direct numerical simulation of turbulent channel flows and wind tunnel measurements in the wake of a single wind turbine. Secondly, we have analyzed the effect of surface roughness and dispersive stresses on the performance of a large wind farm consisting of 50 wind turbines. The results show that the flow resistance generated by ground roughness elements increases the power production of large wind farms by almost 30% when surface roughness changes from smooth to fully aerodynamic rough surface. It was also observed that a significant amount of dispersive stresses persists in the near-surface layer of wind farms.

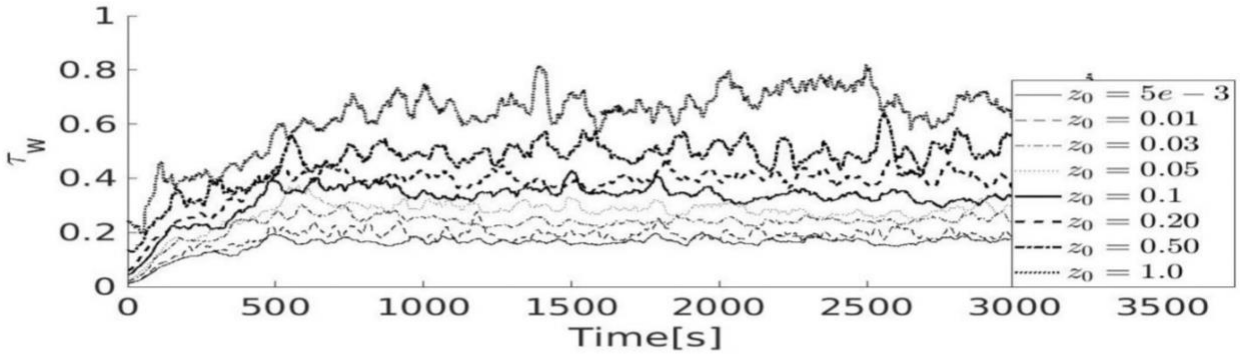

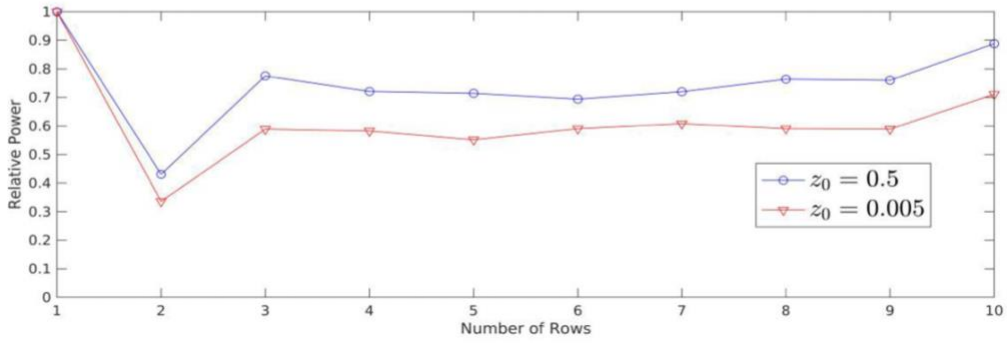

Dynamically Load-Balanced Vorticity-Based Polynomial Adaptation for Transitional and Turbulent Flows

Ramin Ghoreishi, Brian Vermeire

In this paper, a novel dynamically load-balanced polynomial adaptation method for simulations of unsteady flows is introduced. Adaptation is performed based on a non-dimensional vorticity-based indicator. Dynamic Load Balancing (DLB) is employed using the repartitioning routine of the ParMETIS library to optimize the efficiency of the adaptation algorithm. Advection of an isentropic vortex in a periodic domain using the Euler equation is considered to verify the load-balanced polynomial adaptation algorithm. To illustrate the performance of this strategy, three cases have been studied. A case of a three-dimensional circular cylinder at the onset of shear-layer transition regime with Re = 1000 and M = 0.2. A case of a shallow dynamic stall of a three-dimensional SD 7003 airfoil undergoing heaving and pitching motions with Re = 10000 and M = 0.1, pitching motion of $\theta(t) = \theta 0 + \theta e \cos(2\pi f e t + \varphi e)$ around the aerodynamic center, and heaving motion of $y(t) = A\cos(2\pi f e t)$, where $\theta 0$ is the initial/mean angle of attack, θe is the oscillation amplitude, and φe is the phase shift between the heaving and pitching motions. A and f are the amplitude and frequency of the oscillation. The oscillation parameters are set to A/c = 1, a reduced frequency of $fk = \pi fec/U\infty = 0.25$, which results in a period of oscillation of $Te = 4\pi/U\infty$, $\theta 0 = 8^\circ$, $\theta e = -8.42^\circ$, and $\varphi e = 90^\circ$, where $U\infty$ is the free stream velocity. Finally, a case of a NACA 0020 at an angle of attack of $\alpha = 20$, Re = 20000, and M = 0.2 is considered. Time integration is carried out with an optimized Runge-Kutta scheme for all simulations. This adaptation strategy is verified and compared in terms of accuracy and computational cost considering functional targets, namely lift and drag coefficients, of the adaptive and uniform k=5 simulations. Computational cost and scalability of the algorithm are determined by calculating the speed-up factor and efficiency of adaptive simulations. Results demonstrate that the dynamically load-balanced adaptation algorithm can track salient flow features, such as the boundary layer and unsteady wake regions. Qualitative and quantitative results showed equivalent levels of accuracy between the adaptive and high-order solutions with a significant speed-up when adaptation is applied to parallel simulations. We also demonstrate the scalability of the algorithm and the capability of DLB to distribute uniform computational load among processors.

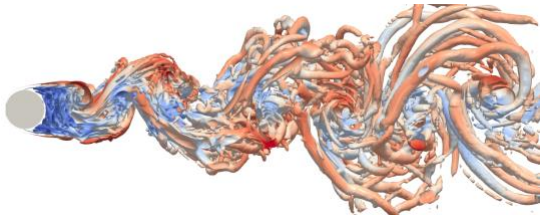

(a) Q-criterion at a minimum lift instant.

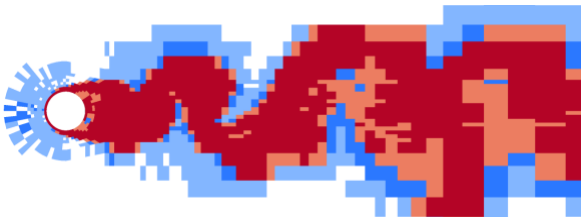

(b) Polynomial degree a minimum lift instant.

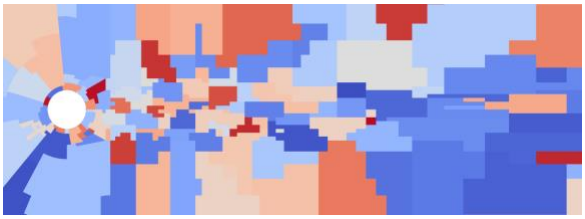

(c) Mesh partition at a minimum lift instant.

Fig. 1. Contours of Q-criterion, polynomial distribution, and dynamically balanced mesh partition for the adaptive computation ($K = 1-5$) based on the vorticity magnitude indicator at the times corresponding to maximal and minimal lift for the three-dimensional circular cylinder with $Re = 1000$ and $M = 0.2$.

A Correlation Based Algebraic Transition Model for Flow Over Rough Surfaces

Mehrdad Noei Yazdian, François Morency

The problem of icing is one of the challenges in the aviation industry which has not been tackled completely. Aircraft icing can affect flight safety in many ways. When the aircraft undergoes icing, due to the changes in the shape and roughness of the surface, the maximum lift coefficient and slope of the lift curve decrease, while the drag and critical stall speed increase. Rough surfaces, such as ice, cause the transition onset location to move upstream and flow become turbulent at lower Reynolds numbers. Since in turbulent flow, the cooling effect increases significantly compared to the laminar flow, it is important to locate the onset of the transition for ice accretion simulation. Several Reynolds-averaged Navier-Stokes transition models exist; However, they were mostly developed over smooth surfaces. For further development over rough surfaces, the SA-BCM (Spalart-Allmaras Bas-Cakmakcioglu with Modifications) transition model was adopted. The SA-BCM transition model is classified as an algebraic or zero-equation model since it employs an intermittency function rather than deriving additional equations for intermittency transport. The underlying model for the SA-BCM transition model is the well-established and validated Spalart-Allmaras (SA) turbulence model. To detect the transition onset location, the turbulence production term of the SA model has been damped with an intermittency function until it satisfies turbulence onset criteria using empirical correlations. First, the experimental results from literature over rough flat plate were utilised as a reference to further develop the SA-BCM model to account for surface roughness. In this experiment, effect of different roughness heights on the transition onset location at a constant free stream velocity has been studied and documented. The empirical correlation mentioned previously has been modified to mimic the same transition location as the experimental results. The model was calibrated against a flat plate with a zero-pressure gradient and various equivalent sand-grain roughness heights. In the next step, NACA0012 airfoil has been chosen to validate the roughness correlation. The validation is done using the same geometry and two Reynolds numbers. The model was able to set the transition point in between the transition region compared to the experimental and other CFD results. However, it was unable to exactly predict the transition onset location and the end of the transition region.

Testing of a Chamfered Wide-Angle Velocity Probe for Characterizing Tornadic Wind Field Using LES

Sameh Elgamal, Mikaela Coello Mena, Haitham Aboshosha, Mohamed Abdelwahab

Tornadoes are a significant disaster event in Canada and North America. There is a need to study the structure and behaviour of tornadoes, in addition to how they interact with the built environment. Moreover, due to the difficulty of field measurement, it is important to simulate this phenomenon in a controlled environment to understand it in a comprehensive manner. Many researchers have attempted to simulate tornadoes by using experimental and numerical methods. However, the characterization of the turbulent tornadic vortices experimentally is a difficult task due to the highly complex tornadic wind field. This study focuses on designing and calibrating a proof-of-concept low-cost velocity probe capable of characterizing complex turbulent flow fields, such as tornadic vortices, acting at a wide range of angles of attack. In the study, a chamfered probe was designed with 16 polyhedral faces allowing for ±120° range of measurement. A mathematical model was developed to account for different angles of attack, including flow impingement between the holes. The probe was investigated using Computation Fluid Dynamics (CFD) employing Large Eddy Simulation (LES) modeling. The probe could predict mean velocities, flow direction and turbulence intensities. the errors in direction was roughly 6°, while the average deviation in the mean wind speed was roughly 3.3%. The error level can be deemed acceptable for wind engineering as well as other industrial applications (e.g. aerospace and automotive applications). These results show initial indication that the chamfered tip shape offers a significant improvement in comparison to other shapes (i.e., spherical shape). The improvement in performance is attributed to the decrease of pressure distribution distortion, lack of irregularities in the numerical 3D model of the probe, and absence of human error. Hence, experimental work is necessary to validate the result of the numerical simulations.

A Multi-Hour Ahead Wind Power Forecasting System Based on a WRF-TOPSIS-ANFIS Model

Yitian Xing, Fue-Sang Lien, William Melek, Eugene Yee

Wind is a clean and renewable energy source with substantial value that is vital for sustainable human development. However, the variability of wind implies that wind power is random, intermittent, and volatile. Wind power forecasting is an effective means of reducing the negative influences of wind power on the reliable, stable, and secure operation of an electrical grid that incorporates wind power systems. For this purpose, a novel multi-hour ahead wind power forecasting system consisting of the optimal combination of statistical, physical, and artificial intelligence (AI) models is proposed in our study. Except for a direct persistence model that is able to provide wind power forecasts directly, an indirect persistence, an autoregressive integrated moving average (ARIMA), and a Weather Research and Forecasting (WRF) model are used to provide wind speed forecasts which, in turn, can be converted to wind power forecasts by using a power curve model. The technique for order of preference by similarity to ideal solution (TOPSIS) is employed to construct a novel 5-in-1 (ensemble) WRF model for wind speed and wind power forecasting. An adaptive neuro-fuzzy inference system (ANFIS) is utilised to determine the power curve model and to correct wind speed forecasts obtained from the 5-in-1 (ensemble) WRF model. By applying a training and test dataset of historical wind speed and wind power measurements obtained from an operational wind turbine in a real wind farm located in North China, a multi-hour ahead wind power forecasting system is proposed consisting of the following components for wind speed and power forecasting over various forecast time horizons: the direct and indirect persistence models for 30-minute ahead forecasts, ARIMA model for 1-hour ahead forecasts, and 5-in-1 (ensemble) WRF model (with corrections obtained from an ANFIS model) for 1.5- to 24-hour ahead forecasts. The results demonstrate that the proposed forecasting system has excellent predictive performance and is of practical relevance.

Numerical Investigation of Flow and Thermal Behaviour in Channels with PCM-Filled Thermal Energy Storage Columns for Potential Application in Photobioreactors

Sameed Akber, Christopher DeGroot, Kamran Siddiqui

Microalgae is a potential source in the production of biofuel. Photobioreactors, which are used in the production of microalgae, normally experience diurnal temperature variations due to changes in the ambient conditions. Microalgae growth is sensitive to temperature variations which affect its productivity. Therefore, the thermal regulation of photobioreactors to minimize temperature variations will result in higher yield of microalgae. The present research is aimed to investigate a novel approach in photobioreactor thermal regulation through the use of latent heat based thermal energy storage, where thermal energy is stored as latent heat in phase change materials (PCM). The present research uses a numerical approach to study the flow and thermal behaviors in a rectangular channel with a set of wall-confined, offset thermal storage columns. The research also aims to investigate the melting behavior of the PCM contained within storage columns, as well as the transient thermal response of the channel flow in the presence of thermal energy storage columns.

The open source CFD software, OpenFOAM, is used to numerically simulate flow in a rectangular channel containing offset PCM-filled columns. The numerical model is validated against experimental data. A parametric analysis is performed to study the effects of various operational and geometric parameters on thermal energy storage within PCM columns, with the aim to optimize the channel geometry and flow conditions to maximize the heat exchange between the PCM columns and the channel fluid.

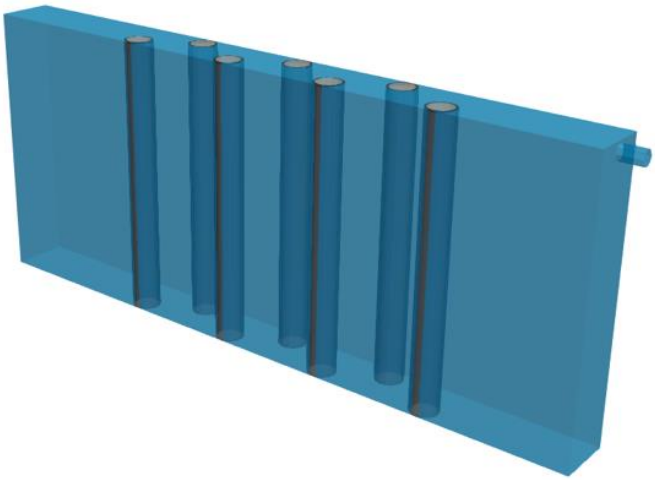

Comparison of Flow and Heat Transfer Characteristics for Solid and Slotted Cylinders Suspended in a Channel

Corey Klinkhamer, Subhadip Das, Ram Balachandar, Ronald M. Barron

Bluff bodies are encountered in many heat transfer applications, such as in pin-fin heat sinks where cylinders are suspended from a heated surface in a confinement channel and submerged in a flowing coolant. A clearance gap is often maintained between the pin-fins and the bottom wall of the device to have an additional surface for enhanced heat transfer. Since pin-fins generally have a circular cross-section, the flow and heat transfer characteristics around two types of circular cylinders are investigated in the present study: a solid cylinder and a slotted cylinder. The height (H) and diameter (d) of the two cylinders are designed to be equal to each other, with an aspect ratio (H/d) of one. A schematic diagram of the cylinder geometry and the flow are presented in Figure 1. The cylinder with the slot has a higher contact surface area with the coolant fluid and is likely to provide a more efficient heat transfer compared to the solid cylinder. For a similar reason, the width of the slot is kept as 10% of the cylinder diameter to maximize this contact surface area. The height of the slot (h) is chosen to be 0.8d leaving a small portion adjacent to the top wall to ensure maximum possible contact area with the heated surface. For both the solid and slotted cylinders, the gap (c) between the lower face of the cylinder and the bottom wall is 0.2d, similar to that used in industrial practice. It is important to note that one of the guiding factors in the flow around the slotted cylinder is the orientation of the cylinder with respect to the direction of the flow. In the present study, three angles of attack (α) 0°, 45° and 90° are used to investigate the variation in the wake generation and the effective heat transfer performance of a single slotted cylinder and these results are compared with those for the solid cylinder. The flow and heat transfer equations are numerically solved and Turbulence is modelled using the Reynolds Stress Transport (RST). A constant heat flux is maintained at the top surface of the cylinder which is attached to the top wall of the simulation domain. Compared to the solid cylinder, the slotted cylinder showed an improved heat transfer performance with up to 5% reduction in the maximum temperature of the heated surface although this value may vary with the magnitude of α. A lower pressure drop was also achieved since the effective cross-sectional blockage is lower for the slotted cylinder compared to that of the solid cylinder.

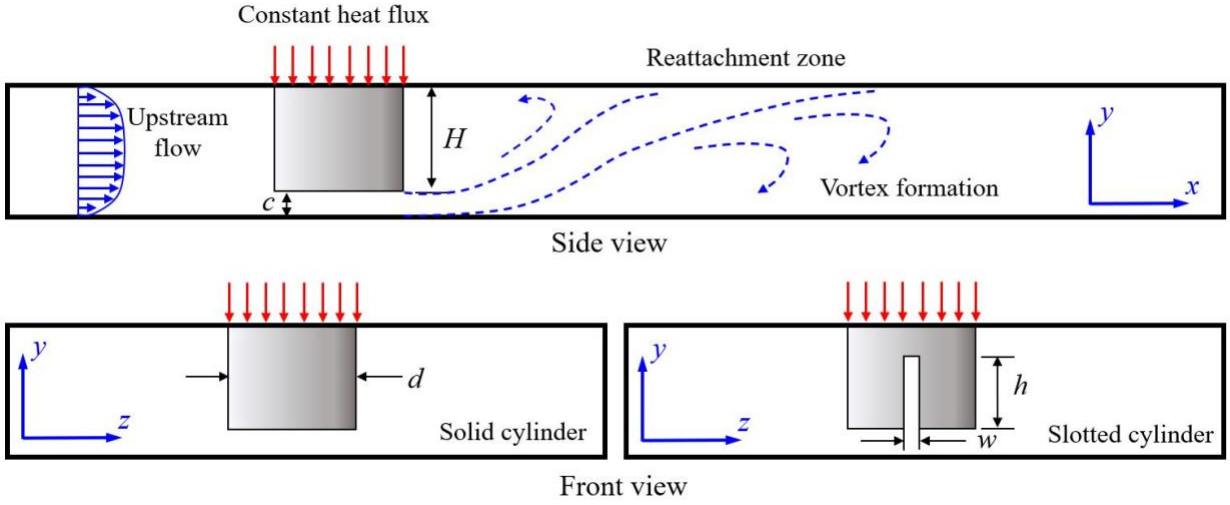

Heat Transfer Mechanism In Particle-Laden Turbulent Shearless Flows

Hamid Reza Zandi Pour, Michele Iovieno

Particle-laden turbulent flows are one of the complex flow regimes involved in a wide range of environmental, industrial, biomedical and aeronautical applications[1]. Recently the interest has included also the interaction between scalars and particles[2], and the complex scenario which arises from the interaction of particle finite inertia, temperature transport, and momentum and heat feedback of particles on the flow leads to a multi-scale and multi-physics phenomenon which is not yet fully understood. The present work aims to investigate the fluid-particle thermal interaction in turbulent mixing under one-way and two-way coupling regimes. A recent novel numerical framework[3] has been used to investigate the impact of suspended sub-Kolmogorov inertial particles on heat transfer within the mixing layer which develops at the interface of two regions with different temperature in an isotropic turbulent flow. Temperature has been considered a passive scalar, advected by the solenoidal velocity field, and subject to the particle thermal feedback in the two-way regime. A self-similar stage always develops where all single-point statistics of the carrier fluid and the suspended particles collapse when properly re-scaled.

We quantify the effect of particle inertial, parametrized through the Stokes and thermal Stokes numbers, on the heat transfer through the Nusselt number, defined as the ratio of the heat transfer to the thermal diffusion. A scale analysis will be presented. We show how the modulation of fluid temperature gradients due to the statistical alignments of the particle velocity and the local carrier flow temperature gradient field, impacts the overall heat transfer in the two-way coupling regime.

References:
1. Brandt, Coletti, Ann.Rev.Fluid Mech 54(2022), Elghobashi, Ann.Rev.Fluid Mech 51(2019).
2. Carbone et al, J.Fluid Mech 881(2019), Saito et al, J.Fluid Mech 931(2022).
3. Carbone, Iovieno, WIT Trans. Eng. Sciences 120 (2018).

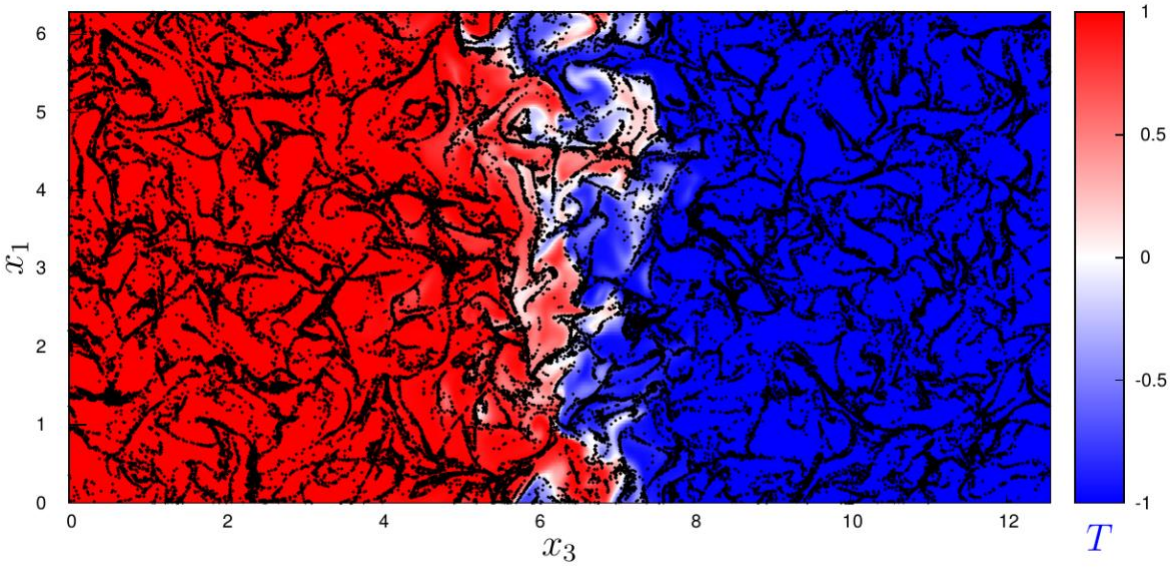

Lethe: An open-source software for CFD, DEM and CFD-DEM

Bruno Blais, Toni El Geitani Nehme, Lucka Barbeau, Victor Oliveira Ferreira, Shahab Golshan

Chemical process plants generally consist of a combination of multiple unit operations which all have a specific purpose: separating components, facilitating a chemical reaction, mixing, transferring energy from one fluid to another, moving fluids. The design of these operations is still mostly based on design heuristics which lead to significant challenges when designing new chemical processes or scaling-up existing ones. These challenges are exacerbated by the occurrence of turbulence, the complex rheology of the fluid or the presence of multiple phases such as a fluid (gas or liquid) and solid particles. Computational Fluid Dynamics (CFD) for the fluid phase, the Discrete Element Method (DEM) for granular material, and their combination (CFD-DEM) enable us to predict the dynamics of these unit operations. This requires high-performance robust models for which the components (linear solver, finite element formulation) are tailored to the application.

In this talk, we introduce a new open-source CFD, DEM and CFD-DEM software: Lethe. Lethe is built upon the well-established deal.II library. It leverages deal.II not only for its state of the art FEM capabilities, but it also makes extensive usage of its high-performance particle tracking module for its DEM solver. We present four very different examples that highlight the challenges that the chemical engineering community face and that can be addressed through CFD, DEM and CFD-DEM simulations:

- The prediction of early turbulent flows.
- The flow of powder in a granular drum.
- The solid-fluid flow in a spouted bed reactor.
- DNS of the flow around one and two spherical particles.

For each of these examples, we discuss the mathematical formulation that we use within Lethe as well as the technical challenges faced when developing the models. We conclude by providing a high-level perspective of the direction in which we are heading, the challenges that we are currently facing and the key lessons that have been learned through this endeavour to develop a CFD/DEM/CFD-DEM software.

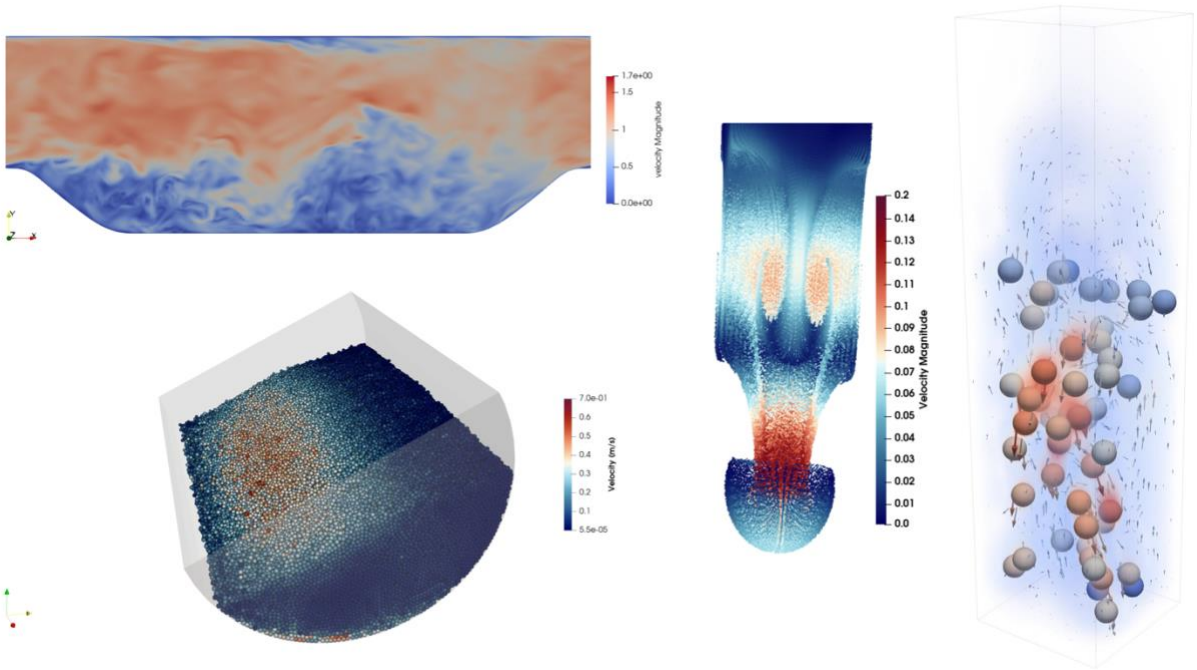

A Cartesian Cut-Stencil Method to Numerically Simulate Two-Dimensional Incompressible Fluid Flow

Yuanming Yu, Ronald M. Barron

A Cartesian cut-stencil (CCST) Finite Difference Method (FDM) that uses quartic functions to locally transform nine-node physical Cartesian stencils into a generic computational stencil (for 2D flow) provides a basis for developing an FD scheme with 2nd-order (upwind) accuracy for the convection terms and 2nd-order (central) accuracy for the diffusion terms in the general transport equation. This setup also permits the option to run a 1st-order upwind scheme for the convection terms. Some benefits of FDM include being easier to understand and implement in a computer code, generally has better convergence properties and provides a straightforward estimator of the discretization error in the form of local truncation error. The primary reason that FDM is not as popular as the Finite Volume and Finite Element methods, especially for commercial use, is that the mesh generation in FDM may be very time-consuming or even fail when dealing with complicated geometries. A desire to overcome this limitation has motivated us to develop the Cartesian cut-stencil method. The quartic function used in the CCST method is designed to transform any non-uniform physical stencil into a corresponding uniform computational stencil. The governing equations for conservation of mass and momentum are transformed into the same form of governing equations but with the computational stencil coordinates. With this arrangement, we can numerically simulate two-dimensional flows even with very complicated geometry. Since the grid system is Cartesian, the difficult task of generating structured meshes is eliminated from the overall solution procedure. The velocity-pressure coupling is achieved by using the SIMPLE algorithm and a momentum interpolation scheme is implemented to avoid non-physical checkboard pressure fields. The results from several 2D test cases will be presented to illustrate the applicability of the CCST approach, including flow in a square lid-driven cavity, a 45-degree slanted-wall lid-driven cavity flow and the flow over a backward-facing step and in a smoothly varying channel. For example, Figure 1 shows the u-component velocity at the middle vertical line for the square lid-driven cavity flow problem. The code will be verified by comparison to well-established results from the published literature. Other features, such as grid convergence, analysis of the local truncation error and grid refinement strategies will be presented.

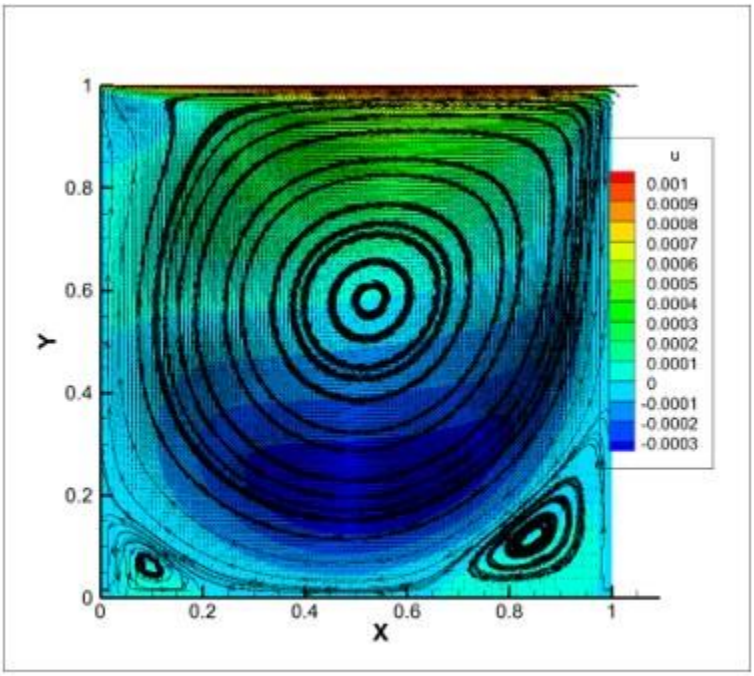

Fig. 1 Streamline pattern with u-velocity component contours (Re =1000, 129x129 mesh)

Paired Explicit Runge-Kutta Schemes for Ansys Fluent's Density-Based Solver

Siavash Hedayati Nasab, Jean-Sebastien Cagnone, Brian C. Vermeire

Recently, a novel time integrator referred to as Paired Explicit Runge-Kutta (P-ERK) methods, has been proposed for solution of locally-stiff systems of equations. This approach allows different Runge-Kutta schemes with different numbers of active stages to be assigned based on local stiffness criteria. In this paper, we develop P-ERK schemes for Ansys Fluent's density-based finite volume solver. Then, we verify that P-ERK schemes obtain their designed order of accuracy using an isentropic vortex case. We then evaluate performance of P-ERK schemes in Fluent's density-based solver with benchmark simulations including flow over a cylinder and turbulent flow over an SD7003 airfoil and T106A turbine blade cascade. We then demonstrate that P-ERK schemes can significantly accelerate simulations and achieve a speed-up factor of up to five when compared to Fluent's default explicit temporal scheme, while maintaining accuracy with respect to reference data.

Multiphase-Heterogeneous Reaction CFD Model of Fast Pyrolysis in a Drop Tube Reactor

Yohannis Tobo, Ashraf Amin, Nader Mahinpey

Reactor insulation, operating temperature, and simultaneous complex chemical reactions make the visualization and experimental measurement of the pyrolysis process inside the reactor challenging task. A reactor scale multiphase flow with heterogeneous reaction and granular flow transport model overcomes the challenges faced in experimental work. In this work a combined heterogeneous reaction, multiphase flow, interphase heat and mass transfer, granular flow, and species transport model with a continuous feedstock flow in a drop tube reactor will be presented. Pyrolysis biofuel yields, biofuel and permanent gas characterization at the reactor outlet, in axial and radial direction will be characterized.

A Numerical Study of a Secondary Clarifier: Transient Effects and Impact of the Density Current Baffle

Anthony Sherratt, Nolan Dyck, Peter Nielsen, Christopher DeGroot, Mark Parker

Clarifiers, also known as sedimentation tanks or settling tanks, are common devices used for separation of solids via gravity. Clarifiers are most notably used in wastewater treatment plants (WWTP) in both primary and secondary settling applications. In secondary settling, the clarifier serves two purposes: (i) separation of solids from the effluent wastewater, and (ii) thickening of the sludge at the bottom of the tank in order to recycle or dispose of the solids. Due to the high cost of installing settling tanks (which can be upwards of 30% of the total WWTP cost) the application of computational fluid dynamics (CFD) models are often applied to predict the performance of the clarifiers in question. In these modeling approaches, the objective is to predict the effluent and return activated sludge (RAS) concentrations under a range of loading conditions the clarifier may be subjected to (e.g. daily average, peak etc.). A limitation to this approach, however, is the assumption of steady state loading, where the clarifier is subjected to a constant flow rate and solids loading rate. In reality, control operators vary the operating conditions of the clarifier in response to hourly variation in raw wastwater flow rates and wastewater quality to ensure the clarifier maintains its performance requirements. As operating conditions are continually changed, the transient response time can vary from minutes to hours, and clarifier CFD models should capture these periods of operation.

The current study investigates transient modeling of clarifiers using two modeling approaches. The clarifier in question will be from the Vauxhaul WWTP in London, Canada. For each modeling approach, the clarifier will be run from the design average loading to the design peak loading and back to design average loading over the course of 24hrs, providing a realistic representation of the loading the clarifier will ungo during operation. To investigate the impact of a geometric change, a density current baffle will be modeled at the outer perimeter of the clarifier, and the simulations will be repeated. This will further highlight the importance of transient modeling before existing clarifiers are modified to increase WWTP capacity. Results will show the effluent and RAS concentrations over time as well as the clear water height for both modeling approaches and geometries.

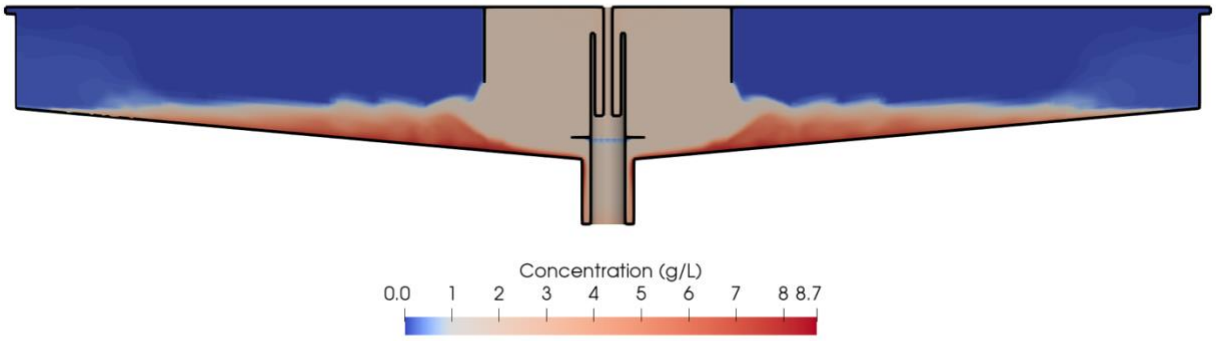

Simulating Flows of Dilute Polyelectrolyte Solutions in Complex Geometries Using a Finite Volume Method

Subham K Das, Burhanuddin Surury, Giovanniantonio Natale, Anne M Benneker

Dilute solutions of charged polymers (polyelectrolytes, PEs), exhibit significantly different flow behaviour when compared to uncharged polymers due to the extra structural rigidity offered by the intramolecular repulsion in PEs. Although the behaviour of such solutions in simple flows has been extensively investigated, studies on their transient flows in complex geometries remain scarce. A robust framework for simulating such flows can provide greater insight into relevant biological and industrial processes (enhanced oil recovery, paints and cosmetics processing, microbial mining etc), and consequently help in optimizing them.

To simulate the flow behaviour of dilute PE solutions in porous media, we use a recently developed rheological model, based on a charged finitely extensible dumbbell with the Peterlin approximation with some modifications for stabilization purposes. The coupled PE-Navier Stokes model, implemented in finite volume CFD solver OpenFOAM can be viewed as an extension of the FENE-P viscoelastic model. The viscoelastic flow solver suite Rheotool, built upon OpenFOAM is used for the finite-volume discretization and solution purposes. The similarity in the structure of our equations with the well-known FENE-P model allows us to use the preexisting discretization and solution schemes in Rheotool and OpenFOAM, appropriately chosen to ensure that the solutions remain stable over a range of physically relevant parameters like the PE charge density, solvent salinity and Deborah numbers. While simulating flows with high elasticity, numerical calculations break down due to the well known high Deborah number problem. We use the log conformation reformulation to stabilize our simulations at high Deborah numbers and investigate flow of dilute PE solutions in idealized porous media, made up of cylinder arrays placed in a channel.

In this work, we for the first time use FVM based numerical simulations to understand the effect of PE charge and salinity of medium on the complex flow dynamics of dilute PE solutions. The applied stabilization methods allow simulations at highly elastic regimes and can be applied to predict the onset of elastic turbulence in flows of PE solutions in porous media. The solvent salinity and PE charge density play an important role in the drag experienced by bodies placed in the flow and onset of elastic instabilities, which can be tuned for specific uses in biomedicine, enhanced oil recovery and macromolecular separations.

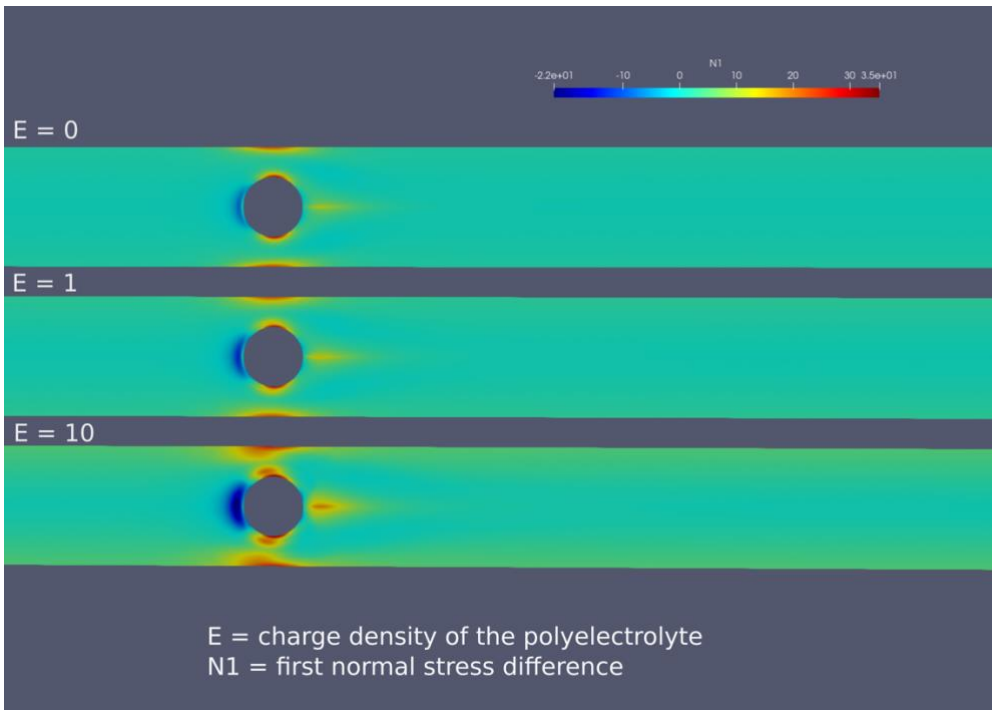

Variational Data Assimilation for the Finite-Volume Method: Examples in 1D MHD Flows

Jose H. Arnal, Clinton P. T. Groth

Over the last several decades significant effort has been devoted to the development of efficient computational fluid dynamics (CFD) schemes for solving hyperbolic systems of conservation laws. Among others, the finite-volume (FV) method has been particularly successful. However, despite the high level of sophistication of CFD schemes, there still arises many circumstances where these methods fail to provide accurate predictions due to uncertainty in model parameters, initial conditions, and boundary conditions. In such cases, observational measurements may prove useful for constraining model uncertainties. A notable instance of this problem occurs in the forecast of space weather. While highly sophisticated models based on the ideal magnetohydrodynamic (MHD) equations have been developed for space weather forecasting, the assimilation of observational in-situ data remains a challenge. In this study, we present the use of a variational data assimilation (DA) scheme to ingest observational data with a second-order FV scheme in one spatial dimension. DA is a set of techniques that formally combines measurements and model predictions to produce estimates with lower uncertainties. In the variational setting, uncertainty reduction is achieved by minimizing a cost function that measures the misfit between the model and observations. A set of adjoint equations pertinent to the FV method are derived and used to drive the minimization routine. Emphasis is given to the algorithm description, while examples of initial-value problems representative of space plasmas are demonstrated. Synthetic observations of the flow-field are generated by sparsely sampling the ideal solution with added noise. A significant level of error reduction is achieved by making use of the proposed DA scheme. Finally, the challenges associated with extensions to three-dimensional computations are discussed.

An Adaptive Time-Step Formulation for Resin Transfer Molding Simulations

Anthony Sherratt, Anthony G. Straatman, Christopher T. DeGroot, Frank Henning

The high weight-specific properties and increased automation potential from utilizing resin transfer molding (RTM) to manufacture high quality carbon fiber reinforced plastics (CFRP) has greatly increased their application in the automotive industry. Manufacturing of RTM components starts with draping, whereby sheets of glass or carbon fibres are cut then laid into the female portion of a rigid, heated mold. The mold is then closed, and resin is injected. After the component is saturated with resin, it is left to cure in the mold for a period which is highly dependent on the operating temperature and the resin being used. After curing, the mold is opened, the part is removed and proceeds to post-processing. The number of steps required to manufacture RTM components has resulted in the increased use of process simulations to optimize each stage of the manufacturing process to reduce the associated experimental costs.

As the complexity of the components increase and more highly reactive resins are investigated the computational costs associated with process simulations are increasing. This is especially apparent when modeling the curing stage, where the accuracy of the predicted cure rate and resulting heat release is highly dependent on the imposed simulation time-step size. The current study investigates this limitation by first determining the maximum time-step that can be set for a curing simulation (for a given resin) using a custom version of the open-source computational fluid dynamics software OpenFOAM. This is done by modeling 1D curing (i.e., no influence of mold temperature) where the resin is allowed to cure from 0% to 60% using constant time-steps ranging from 0.00025–5 [s]. The numerically predicted temperature rise can then be compared to an analytical solution of the temperature rise, which shows that the maximum possible time-step is 0.01[s] to ensure a temperature rise error of less than 1%. A formulation is then proposed which allows the time-step to vary depending on a fitting parameter, the maximum global cure rate, and minimum global cure degree within the mold. The unbounded nature of the formulation requires that an upper limit on the time-step also be set. After an optimization study, it is found that using a value of 0.01 for the fitting parameter and an upper limit of 0.075[s] for the time-step resulted in a 10x reduction in the computational time when compared to using a constant time-step of 0.01[s].

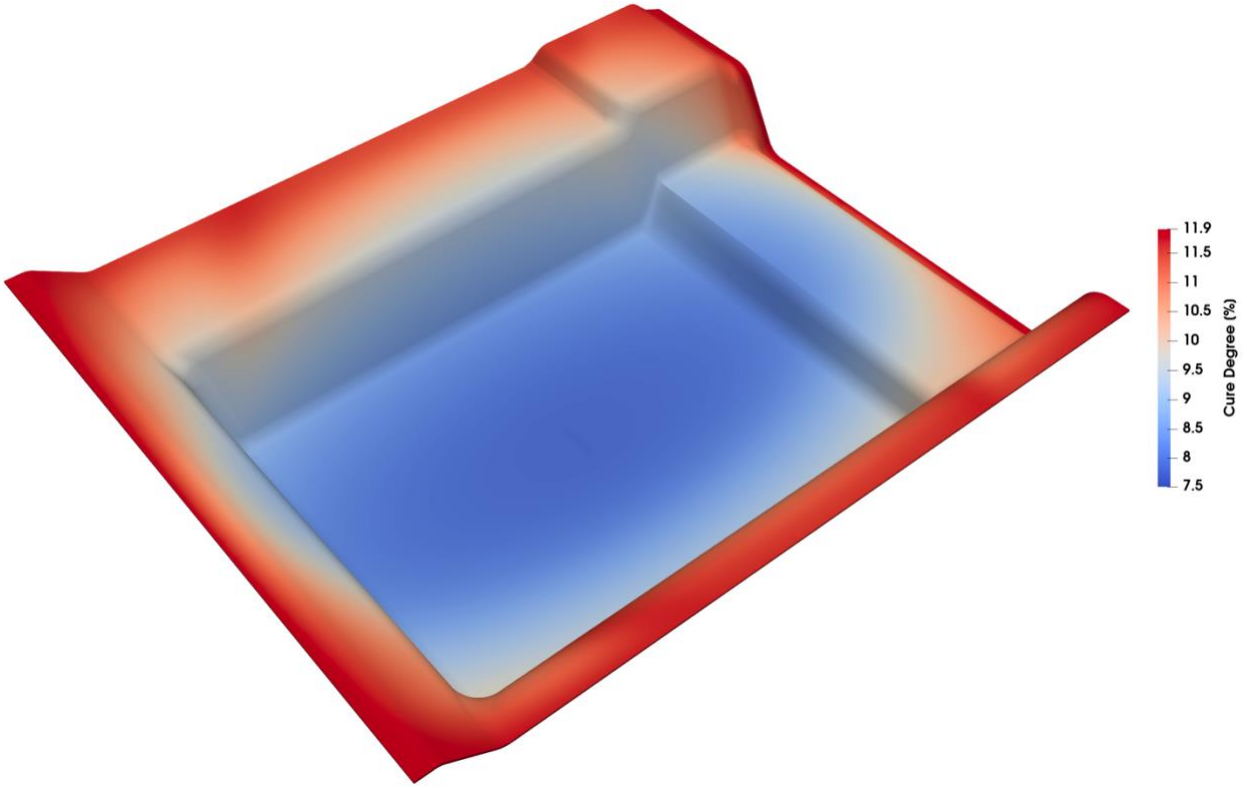

A High-Order Unstructured Solver for Moving and Deforming Domains using the Entropically Damped Artificial Compressibility Method

Marie-Pier Bolduc, Ramin Ghoreishi, Brian Vermeire

A wide range of applications require accurate, efficient, and stable solutions for incompressible flows around complex moving and deforming geometries. For example, hemodynamics, hydrofoils, and bio-locomotion of fish and other underwater creatures. These problems can prove to be particularly challenging due to large geometric deformations and translations, and because they inherently require unsteady solution techniques capable of resolving a wide range of length and time scales. A suitable solution technique is the flux reconstruction (FR) method, a high-order unstructured spatial discretization that uses an element-wise polynomial representation of the solution. In the context of moving and deforming domain (MDD), this method has been validated with the Arbitrary Lagrangian-Eulerian (ALE) form of the compressible Navier-Stokes equations by Ghoreishi & Vermeire and Liu et al. However, the incompressible Navier-Stokes equations remains to be validated.

The entropically damped artificial compressibility (EDAC) method offers a pressure-dampening alternative to conventional Poisson's or artificial compressibility methods (ACM). EDAC uses an artificial compressibility parameter, similar to the ACM, but does not require pseudo-iterations to converge the pressure field. Thus, EDAC can be formulated as a fully-explicit method, which is suitable for acceleration on modern hardware architectures.

While EDAC has previously been successfully tested using various finite-difference methods and FR methods, its implementation combined with ALE on MDD remains to be seen. This research serves to close this gap by using the EDAC solver with the ALE implementation in the High-Order Unstructured Solver (HORUS) developed by the Computational Aerodynamics Lab at Concordia University. First, the method of manufactured solutions will be used to verify the implementation of the solver via an order-of-accuracy criteria. Next, the double shear layer is used to assess the ability of the scheme to preserve the physics at high order and determine the impact of the artificial compressibility factor. Then, the accuracy of EDAC is further illustrated through simulation of flow over an oscillating cylinder at two different flow settings and of dynamic stall of a 2D NACA 0012 airfoil undergoing heaving and pitching motions. Results demonstrate that artificial compressibility factors on the order of 0.025-0.1 were required to recover the reference solutions on MDD.

Prediction of the Acoustic Refraction Through Shear Layers with Deep Neural Networks

Antonio Alguacil, Michael Bauerheim, Lorenzo Becherucci, Marc C. Jacob, Stéphane Moreau

A novel acoustic propagation methodology is developed, based on a surrogate model able to propagate acoustic waves in complex flows. The problem of acoustic refraction by a sheared flow is considered. In particular, the academic configuration of acoustic propagation of an oblique plane wave in a thick planar shear layer is considered. A database is generated with the LES solver AVBP consisting of runs with different incident wave angles. Depending on this angle, full transmission, partial transmission and reflection, or full reflections are obtained. The reflection and transmission coefficients also compare favorably with an asymptotic analytical model for propagation through a thick shear layer.

The database is employed to train a UNet convolutional neural network that predicts the time propagation of the fluctuating pressure in an autoregressive way, given some initial conditions and acoustic source characteristics.

The trained neural network is used to make predictions for the acoustic propagation. First the capacity to predict in the same range as the database is evaluated (is the network able to learn the training data?), then, and more importantly, the capacity of the network to extrapolate outside its training range (e.g. in terms of shear layer parameters M, δ) is assessed for the major different propagation regimes highlighted above. Good results are obtained for the full transmission case, whereas larger errors are observed for the full reflection case. Intermediate results are found for the partial transmission and reflection, with again most of the errors located on the reflection side. Further investigation is therefore needed to understand why the neural network has more difficulties with reflection from the shear layer.

Validation of Artificial Intelligence Approach to Anomalous Bioaerosol Trigger Detection Using Synthetic Data from a Computational Fluid Dynamics Simulation Environment

Hsuan-Han Huang, Eugene Yee, Fue-Sang Lien, Andrew Wong

A network of point-trigger (optical) sensors can be used to continuously monitor the ambient atmospheric environment for the possible presence of a potential threat aerosol. If an anomalous threat aerosol is detected in the ambient air, then the point-trigger sensors activate a bio-collection and identification system to determine if the anomalous aerosol is a true bio-agent. In this process, the trigger algorithm is a key-enabling component of the point-trigger sensor network for the detection of an anomalous bioaerosol in the ambient environment.

To address the latter problem (viz., trigger algorithm), we need to first develop a “realistic” simulation environment owing to the fact that the testing of aerosol triggers in the real world is a very challenging and expensive undertaking. This simulation environment consists of two components: (1) the transport and dispersion of the dynamically evolving threat bio-agent from the source to receptor using large-eddy simulation; and, (2) development of a stochastic time series model to represent the natural and complex background aerosol (interference or clutter). The synthetic data generated from this simulation environment are used to test a number of different predictive analytics-based (artificial intelligence) “smart” trigger algorithms for anomaly detection of a potential threat aerosol in a noisy dynamic ambient environment for various signal-to-clutter ratios (SCRs) (including very low SCRs corresponding to cases where the ambient particle concentration greatly exceeds the threat aerosol concentration). The “smart” trigger algorithms include one-class SVM, isolation forest, LSTM neural network and, TadGAN generative adversarial network.

The capability of these state-of-the-science machine learning anomaly detection algorithms to unravel the subtle functionalities and relationships in the sensor data in order to differentiate normal (background clutter) and anomalous behavior (non-conforming or emergent patterns in the data not consistent with expected behavior) is evaluated rigorously. In particular, for each analytics-based trigger algorithm, the anomaly detection performance is evaluated in terms of a number of performance metrics for the continuously-operating trigger sensors. These performance metrics include the ROC curve which is used to represent the relationship between critical performance characteristics such as probability of detection, probability of false alarm, and system sensitivity.

Aeroacoustic Shape Optimization Using Large Eddy Simulation

Mohsen Hamedi, Brian Vermeire

Aircraft noise is a general nuisance in urban environments, has been shown to cause a range of health problems. The International Air Transport Association (IATA) predicts that total air transport could double, following present trends, over the next two decades. This is expected to greatly increase the amount of noise pollution and, therefore, next-generation aircraft must be designed to be as quiet as possible.

This research study the performance of high-order methods for aero-acoustics prediction and optimization of turbulent flows and associated far-field noise. The high-order Discontinuous Galerkin (DG) method, recovered via the Flux Reconstruction (FR) approach, is used for spatial discretization, along with the Implicit Large Eddy Simulation (ILES) for turbulence modelling.
In general, there are two approaches for Computational Aero-Acoustics (CAA). The first approach, the direct approach, is the most accurate and computationally expensive approach. In this approach, the sound field is computed together with the unsteady turbulent flow field using CFD techniques. The sound is predicted at any point by computing the acoustic pressure directly from the CFD results. Thus, the observer must be inside the computational domain. However, the obtained CFD numerical solution is used as input to the acoustic solver in the hybrid CAA approach, where the sound pressure level is computed. Different analogies are used in the hybrid CAA approach, and in this study, the Ffowcs Williams and Hawkings (FW-H) formulation is used.

In the current study, an acoustic solver is developed based on the FW-H formulation and is verified using the analytical monopole and dipole equations. Then, a monopole is placed in a quiescent flow, and the Euler equations are solved as the validation of the FW-H framework.
Finally, two aero-acoustic benchmark problems are considered in two dimensions. First, flow over a square cavity is studied, and the length of the cavity is optimized to have the tonal peak within a pre-specified range of frequencies. The Mesh Adaptive Direct Search (MADS) method is used as the gradient-free optimization technique. The flow over an airfoil is then investigated in two dimensions, and the airfoil shape is optimized to minimize the tonal peak. The direct CAA approach is used for the benchmark problems, and the results show the capabilities of the MADS optimization technique in conjunction with the high-order FR approach.

Flow-Induced Vibration of Cylinder-Plate Appendage at Low Reynolds Number

Ying Wu, Fue-Sang Lien, Eugene Yee

Fluid-induced vibrations (FIV) of cylinder, mainly referring to vortex-induced vibration (VIV) and galloping, is a classical bidirectional fluid-structure interactions (FSI). Considering its great potential damage to engineering structures, a rigid splitter plate is often attached behind fixed cylinder as a wake stabilizer to suppress the structural oscillation. However, an unexpected dynamic response of the elastically supported cylinder-plate system has been repeatedly reported in experimental and numerical works, that is the transition from VIV to galloping with appropriate conditions. From the perspective of fluid energy harnessing, this unique aeroelastic behavior qualifies cylinder-plate to be a natural energy harvester utilizing the mutual effect of VIV and galloping, in which the splitter plate is used to strengthen the oscillation. In the present work, the dynamic instability of an elastically-mounted cylinder with splitter plate assembly allowed to move freely in the cross-flow direction is numerically investigated at low Reynolds number using OpenFOAM. In order to possess an overall understanding on the influence of plate on cylinder, a systematic simulation is carried out to cover a wide range of plate length, LSP=0-4D, and the reduced velocity, Ur=0−30. While other fluid and structure properties remain the same, including mass ratio m^*=10, damping ratio ζ=0, Reynolds number of 100, etc. Firstly, the dynamic characteristics of cylinder-plate with different plate lengths is generally described in terms of oscillation amplitude, frequency response, and aerodynamic forces. Secondly, emphasis is laid on analyzing a few key plate lengths having completely different response modes or close to transition, and representative reduced velocities such as VIV and galloping onset. In an attempt to reveal the underlying mechanism of the influence of splitter plate on cylinder, we mainly focus on the relationship between vibration displacement and the fluid force respectively acting on cylinder and plate, including comparing the shape of time history curves, phase angle, power spectral density (PSD), etc. Thirdly, the wake evolution is studied by intuitively observing the vorticity field during single period of vibration.

Based on the analyses of combined VIV and galloping, at last, a passive control strategy for cylinder-plate energy harvester is proposed to realize the optimal power performance by real-time adjusting the plate length based on inflow speed.

Aeroacoustic Investigation of Automotive Engine Cooling Modules Using the Lattice-Boltzmann Method

Safouane Tebib, Athreya Ballapur Jayasimha, Stéphane Moreau , Bruno Desmory, Manuel Henner, Adrien Mann, Charles Luzzato

The present study focuses on the aeroacoustic aspects of engine cooling modules used in both classical and electrical vehicles (EV). These modules aim at cooling down the engine in combustion cars and the electrical components in EVs. During the fast charging process of such vehicles, a huge amount of power is transferred to the battery in a short period of time that causes its overheating. Several fans are installed in order to cool down these components, thus multiplying the noise sources that are propagated both outside and inside the cabin and can be harmful for the pedestrians as well as the passengers. Lattice-Boltzmann simulations are performed on both the classical and the electrical module in order to understand the noise mechanisms and highlight the difference between them. The results are compared with the experimental measurements achieved in the anechoic wind tunnel at Université de Sherbrooke. Medium grid simulations have shown a good flow behavior and establishment for the operating point considered with some possibly noise sources localisation. The direct farfield noise computations also show a good overall match with the experimental data. Modal analysis performed on the electrical module shows the duct role in the acoustic response of the module to an external noise source that mimic the car environment.

Effect of Flow Coefficient on Performance of a Linear Compressor Cascade with Tip Gap

Ahmadou Bamba Drame

The presence of a clearance between the blade tip and the casing wall in a rotating machine is necessary for its proper operation. However, its existence is a major source on unfavorable flow phenomena so-called tip leakage flow. This tip leakage flow (TLF) is favored by the pressure difference between the pressure side and the suction side that increases when the flow rate across a machine is decreased. At the clearance exit, the TLF interacts with the main flow and rolls up to form the Tip Leakage Vortex (TLV) . Then, it diffuses and can eventually merge with the blades wakes and it is a major source of performance deterioration for axial turbomachinery. However, theses mechanisms depends on several parameters such as: the mass flow rate, the tip gap size, and the blade loading. The present study will investigate the influence of the mass flow rate though a cascade with a fixed tip gap. The purpose of this study is also to clarify the effects of decreasing the flow coefficient close to the optimum point on the performance parameters.

In this context, the TLF with different mass flow rate is simulated using the Reynolds Average Navier-Stokes method. The investigated simulation is based on the linear compressor cascade with tip gap that has been measured in the low-speed wind tunnel at Virginia Tech. The Reynolds number based on the chord is 400,000 and the mach number based on the inlet velocity is 0.07. The size of the clearance is 4mm and represents 1.6% of the chord (C=254 mm). The provided figure detail the investigated linear cascade and the parameters that control the boundary conditions. The simulations are then performed with the high resolution advection scheme of ANSYS CFX solver incompressible. The wall resolution wall units y+ is about 3 to 5. The turbulence model k-ω shear-stress transport model is used.

In a first step, the TLF and the topology of the TLV related to the presence of the tip gap will be analyzed for the baseline configuration at optimal operating condition. The simulations results will be compared with the experimental results available in the literature. Then, a general analysis of the losses generated as a function of the flow coefficients will be studied. The tip TLV trajectory, its core velocity deficit, and its circulation will be determined for the different simulated mass flow rates. These vortex parameters and the measured losses will serve as the basis of a new model for cascade design and performance tools.

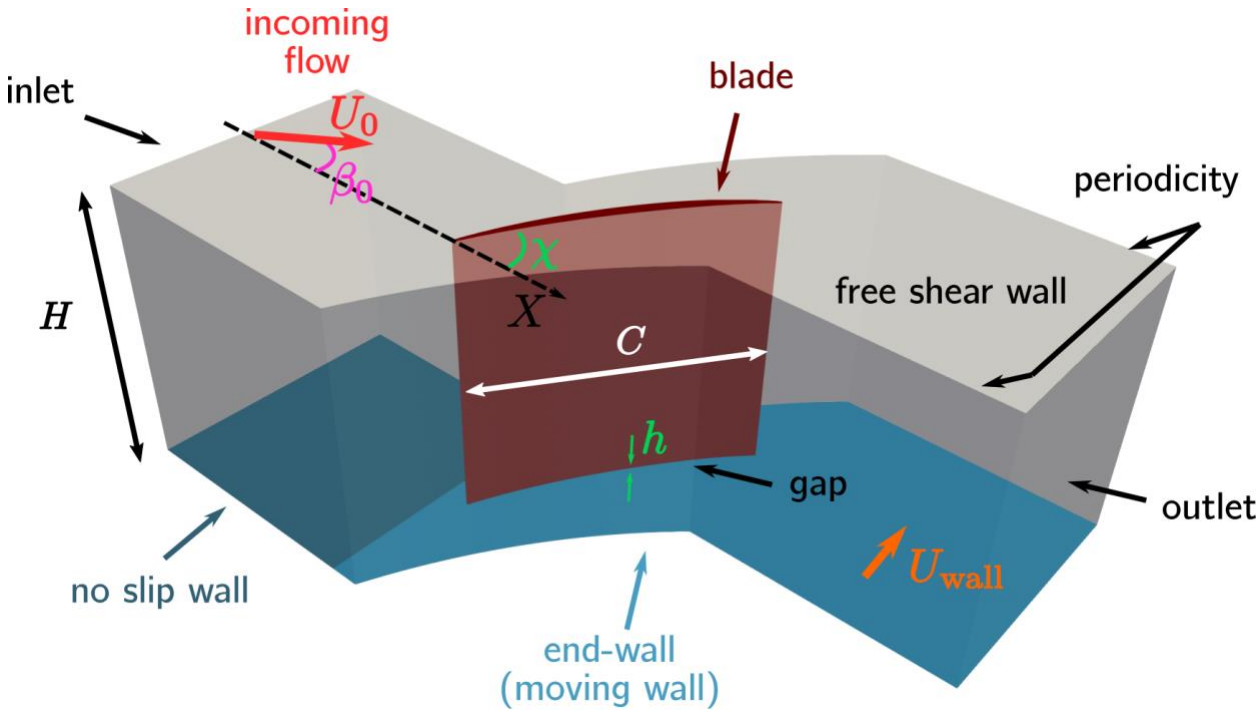

The Effects of Ideal Gas Properties on Losses Through Inflow Control Devices Operating Near and at Choked Conditions

Jean-Luc Olsen, Carlos F. Lange

Inflow control devices (ICDs) are used widely in Alberta to decrease both the economic and environmental costs of steam assisted gravity drainage (SAGD) based oil extraction. An ideal ICD is highly fluid selective: it creates pressure drop primarily through mechanisms that are sensitive to the fluid properties unique to undesired fluids, while creating little pressure drop through mechanisms strongly dependent on the fluid properties of desired fluids. One goal of our research group is to develop better criteria for comparing ICD designs that capture the ICD's ability to be fluid selective towards allowing viscous bitumen while restricting water, steam, and solvents which tend to flow at higher velocities. Previous work has focused on normal SAGD operating conditions, which are incompressible flows of bitumen and water.

Current work is expanding into the compressible and choked flow regimes using ideal gas approximations of steam and butane. This study explores the effects of individual fluid properties on pressure losses of ideal gases flowing through various ICD geometries. Also being explored is the effect of minor geometry smoothing on simulation stability which allows for the use of higher order advection schemes. Future work will be developing a mathematical model for the general relation between mass flow rate and overall pressure drop. Steady state, total energy, and SST turbulence models are being used in ANSYS CFX to simulate the flows.

This study presents performance curves from multiple ICD geometries with three variations of an ideal gas flowing through them. The variables changed between each gas are the molecular mass, which affects the density of the gas and the Reynolds number of the flow, and the specific heat ratio, an important variable in the mass flow vs pressure correlation. Changes, or lack thereof, in the mass flow vs pressure performance as a result of changing the fluid are discussed and compared to theoretical predictions. For our flow cases, an increase in the molecular mass without a change in the specific heat ratio is shown to at most slightly decrease losses, while a decrease in the specific heat ratio is shown to decrease losses a small amount. Lastly, the use of small fillets on sharp edged geometries that previously would only converge using a pure upwind advection scheme is shown to allow the use of blended upwind and central differencing schemes with small effect from the geometry on the overall mass flow results.

Hydrogen Risk Analysis During Severe Accidents in a 1000 MWe Nuclear Power Plant

Amponsah Joseph

In the course of a severe accident in a light-water nuclear reactor, hydrogen production can be released in large quantities during zirconium-water interaction. This in turn disrupts the integrity of the containment and as a result raises a combustion hazard in the nuclear facility, leading to the failure of surrounding buildings. Several European countries have adopted mitigation strategies to prevent the gas explosion hazard by the use of passive autocatalytic recombiners (PARs). Research works on accident sequences show that, despite the installation of PARs, it is difficult to prevent at all times and locations, the formation of a combustible mixture that hypothetically leads to local flame detonation. New research and development (R&D) projects recently launched are being used to understand better the phenomena associated with the combustion hazard and to address the issues highlighted after the Fukushima Daiichi events such as explosion hazard in the venting system and the potentially flammable mixture migration into spaces beyond the primary containment.

In this paper, hydrogen generation and distribution concerning its concentration were analyzed through a simulation of a 1000MWe nuclear power plant with a CFX model. Evaluation of hydrogen risk and recommendation mitigation strategies to prevent future accidents were also touched on. The effect of using passive autocatalytic recombiners (PARs) as a mitigation system was evaluated by comparing the results with and without installing thirty-nine PARs.

Ansys CFX code was used in calculating hydrogen distribution in the vessel and the interpretation of the results was possible with Ansys's CFD Post application package. The expected outcome of this research work was to ensure the volume concentration of hydrogen generated with 100% fuel clad-coolant reaction was distributed in the containment uniformly and that it should not exceed 10% during or after a severe accident using a CFX code. After the simulation was run it was clear the final hydrogen percent for the model without recombiners was 17.85% (mass of 1600 kg) and the simulation model with recombiners was 9.72% (mass of 440 kg). Obtaining the prime expectations stated in the initial chapter of this thesis report.

Applied CFD Modeling to Protect Environment and Support Energy Industry

Vandad Talimi, Lei Liu, Shafiul Mintu, Prem Thodi, Jonathon Bruce, Tony King, Freeman Ralph

Computational Fluid Dynamics (CFD) has been widely used by industry in concept development, design optimization, system performance enhancement, failure assessment, and verification and validation of new ideas. Industries have benefited from the recent developments in software and hardware, and now can complete CFD models with desired accuracy in a timely manner. There are several published best practices derived from these experiences.

Atlantic Canada, and especially Newfoundland and Labrador, has recently seen major growth in energy industry, both renewables and oil and gas. C-CORE, as a non-for-profit applied R&D organization has completed several CFD modeling works to support the recent industrial activities in the province as well as nationally and internationally. These projects were in the areas of offshore renewable energy production, pipeline thermal management, iceberg hydrodynamics, oil spill mechanical recovery enhancement, carbon capture, environment protection using underwater air bubbler systems, flow assurance, multiphase flow modeling, and gas hydrate management to name a few. The authors present an overview of CFD modeling approaches utilized in these projects, quality control processes used to ensure the validity of the models, and the main lessons learned which can help CFD engineers increase their modeling success.

Darwinian MAVs: The Biomimicry of a Hybridization of Small Birds' Flight Patterns in the UAV Context

Benjamin D. Fedoruk, Amanda M. Showler, Neel S. Shah

Darwinian evolution has yielded adaptations of small birds to their environments. Leveraging these abstractions to create biomimetic MAVs can significantly improve UAV technology. Hybridizations of flight patterns of several small birds are isolated for a selection of use cases, including environment, load and manoeuvrability. The MAV status of the birds is affirmed by calculating their Reynolds numbers. The ensuing discussion applies the hybridizations to the UAV context. Future research should construct and simulate models under varying conditions.

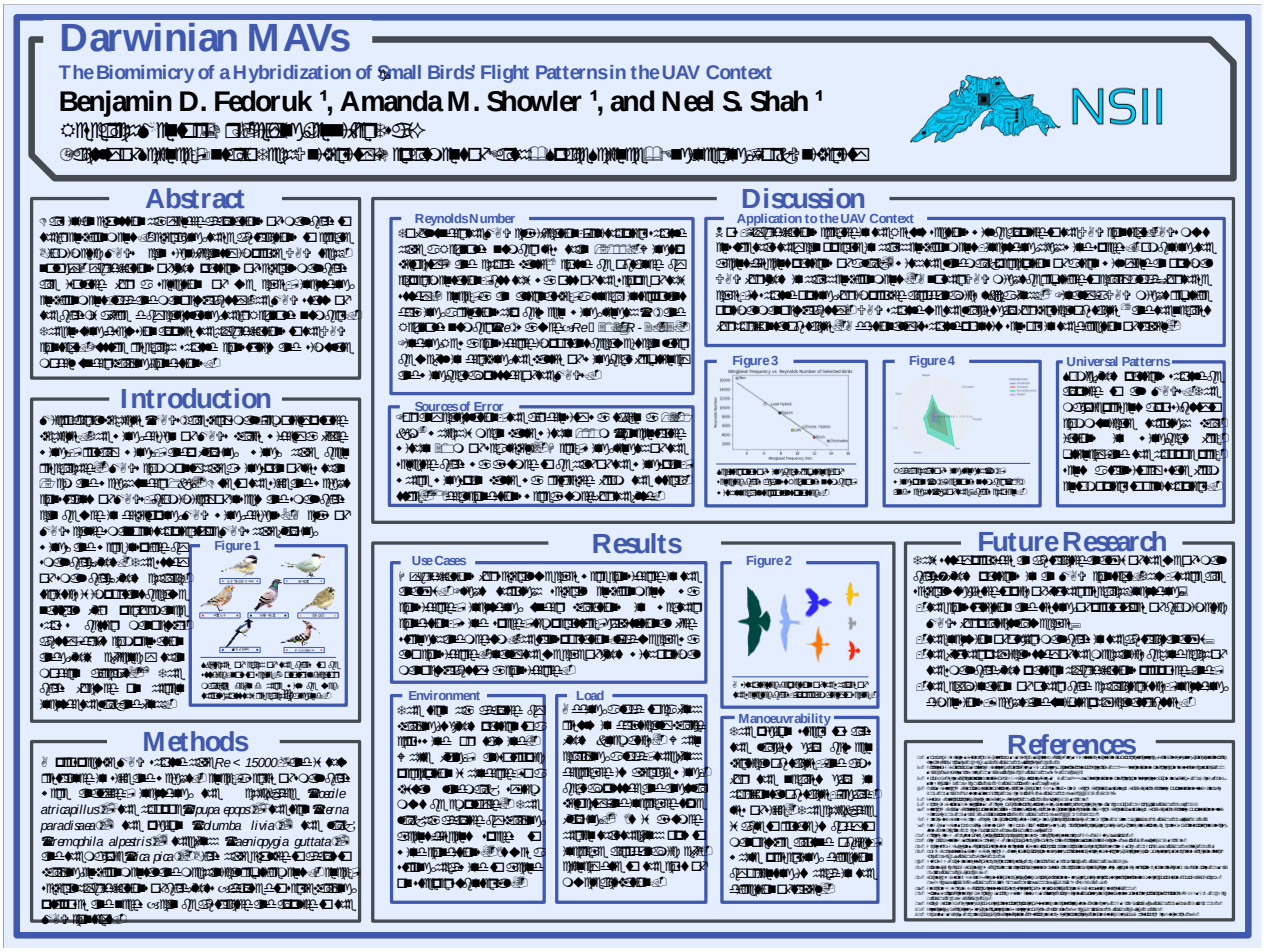

Assessment of Iterative Solvers for Large Eddy Simulation of Wind Farms

Collins Bekoe, Jagdeep Singh, Jahrul Alam

This study presents a numerical investigation of the turbulent flow in and around wind farms. The 3-D Navier-Stokes equations are discretized to characterize the flow in wind farms. We have proposed a scale-adaptive large eddy simulation (LES) method. This LES employs vortex stretching to combine scale similarity with the Smagorinsky model. The skew-symmetry of the non-linear advection is locally preserved. Finally, two linear systems of equations are solved at each time step. Two linear system matrices, one for velocity and one for pressure, are obtained after discretization of the Navier-Stokes equations. Linear system matrices play a vital role in determining the overall cost of the numerical methods. Therefore, the present article analyzes and assesses iterative solvers for large wind farms for effective simulation results. The performance of iterative methods for wind farm simulations is investigated by comparing the Krylov subspace and the multigrid methods. We performed several numerical tests with different preconditioners for the Krylov subspace methods and observed that the Krylov subspace method with multigrid as a preconditioner needs relatively less number of iterations with less computational time. The scaling of the Krylov-multigrid solver is verified by investigating the speedup with respect to the number of processors. The results showed that the speed up is efficient up to 256 processors, where a further increase in the number of processors to 1024 leads to a decrease in the speedup as well as the efficiency.

Solver	Pressure Error	Velocity Error	Average Iter	Time
Krylov	3.01×10^{-6}	6.47×10^{-5}	568.32	402.00
Krylov-FDIC	8.5×10^{-7}	8.9×10^{-7}	261.00	308.00
Krylov-DIC	8.5×10^{-7}	8.9×10^{-7}	255.00	289.87
Multigrid	4.6×10^{-7}	9.7×10^{-6}	8.97	130.00
Krylov-multigrid	6.22×10^{-6}	1.38×10^{-5}	1.00	118.94

Table 1: Comparison between the multigrid and Krylov subspace method with Fast diagonal-based incomplete Cholesky (FDIC), diagonal-based incomplete Cholesky (DIC) and multigrid as preconditioners to analyze the pressure and velocity errors. Table also shows the average iteration per time step and simulation time.

No. of Processors($\mathcal{N}_p$)	Time (sec)	Speed up = T(1)/T($\mathcal{N}_p$)	Efficiency
1	17.1270	1	1
4	4.6921	3.65	0.9125
8	2.6595	6.44	0.8050
16	1.7408	9.84	0.6149
24	1.6296	10.50	0.4379
40	0.7584	22.58	0.5646
64	0.6035	28.38	0.4434
96	0.3581	47.83	0.4982
128	0.3351	51.11	0.3993
256	0.2762	62.00	0.2422
512	0.3443	49.74	0.0970
1024	1.3640	12.56	0.012

Table 2: Table shows the scalability of Krylov-multigrid solver, where time is the average execution time per time step and consequently speed up effect and efficiency are computed for each number of processors ($\mathcal{N}_p$).

Evaluation of Wind Flow Over Natural Complex Terrain Using Computational Fluid Dynamics: Case Study for Montreal, Quebec, Canada

Mohamed Hamdy, Tarek Ghazal, Haitham Aboshoshsa

Several wind engineering applications necessitate precise and resolutely computational fluid dynamics (CFD) simulations, such as modeling the wind flow across complex terrain. Historically, only a few CFD studies of wind flow around cities surrounded by complex terrain have been conducted. Consequently, this paper offers a CFD case study on the city of Montreal located in Quebec, Canada with field measurement validation. A model that accounts for both terrain and topographical effects was developed and CFD simulations were conducted using the 3D Reynolds–averaged Navier–Stokes (RANS) equations and a revised k–ε model. Afterwards, the developed model was applied to the city of Montreal to evaluate the mean wind flow patterns around the city's complex terrain. Simulations were conducted for 36 different wind angles of attack, and the developed model has shown a percentage of ~7% root mean square error (RMSE) when compared to the historical measurements obtained from meteorological stations.

Numerical Investigation of the Noise Radiated by a Helical Darrieus Vertical Axis Wind Turbine in Operational Regime

Kartik Venkatraman, Stéphane Moreau, Julien Christophe, Christophe Schram

The growing need for reducing carbon emissions has spurred an interest in siting of small wind turbines in urban areas with high wind potential such as building rooftops. Darrieus vertical axis wind turbines (VAWTs) have been shown to well suited for such turbulent wind conditions with constantly changing wind direction. However, typical Darrieus VAWT architectures such as the classical (Troposkein) and straight bladed turbines (H-Darrieus) show a poor aerodynamic performance. An alternative concept is the helical VAWT first proposed by Gorlov in 1995. This architecture has shown to provided low torque fluctuation per rotational cycle, thereby minimizing the problems due to fatigue and vibrations and power output. Moreover, manufactures of helical VAWTs such as Quiet Revolution (QR6) also claim that the design provides a lower noise signature compared to standard H-Darrieus turbines. Accounting for the 3D flow and complex flow structures requires a high-fidelity simulation capturing the key flow structures close to the blade and the interior of the rotor. However, very few 3D high-fidelity simulations exist in the literature for helical VAWTs and are primarily focused on their aerodynamic performance. This study aims to address the research gap on the aerodynamic and noise characteristics of a helical VAWT in its operational regime. A three-dimensional hybrid Lattice Boltzmann/Very Large Eddy simulation (LBM-VLES) model is setup using the solver PowerFLOW to simulate a helical Darrieus vertical axis wind turbine in the operational (maximum efficiency) regime and compared with available experimental data from Weber et. al (2017). Simulations are performed for three different blade helix (sweep) angles – 45°, 60° and 120°. The sound pressure level at a given observer position located 1 m away is predicted using both a direct approach and a FW-H analogy. The predicted noise spectrum for the turbine with helix angle 45° shows a good agreement with experimental data for both the tonal and broadband components. A decrease in overall noise levels is seen with increasing helix angles at the same observer position. The flow physics and noise directivity of these machines shall be further investigated to confirm the possibility of using swept helical blades as a noise mitigation strategy for Darrieus VAWTs.

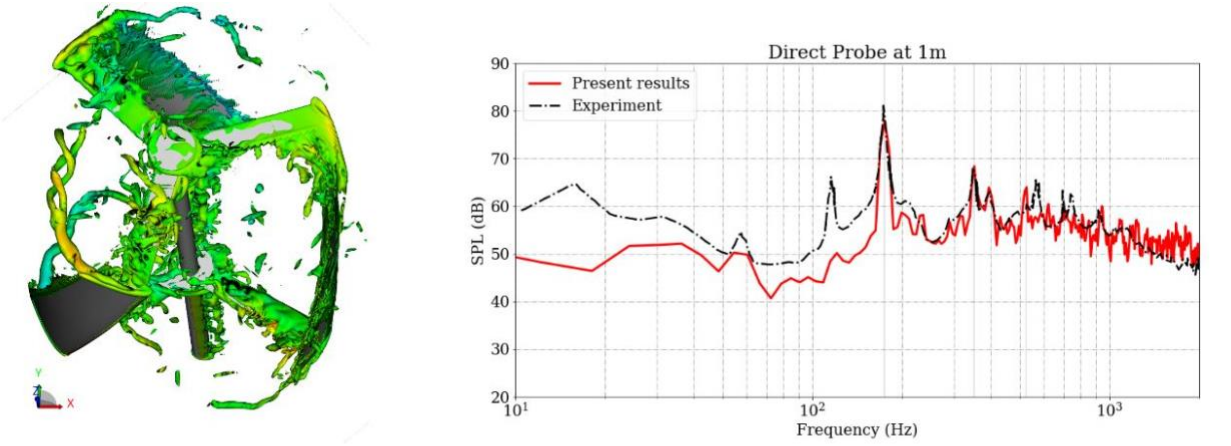

(a) Flow structures (b) Noise spectra

Figure 1: (a) Iso-surfaces of Q-criterion to visualize flow structures, shown the 3D flow and tip vortices. (b) Comparison of direct noise spectra with experimental data from Weber *et al.* (2017)

Liquid Jet Impingement Heat Sink for Power Electronics Cooling with Rib Enhanced Heat Transfer

Corey Klinkhamer, Subhadeep Mondal, Lakshmi Varaha Iyer, Ram Balachandar, Ronald M. Barron

With the ongoing shift to electrified vehicles, comes a great demand for on-board power electronics that are more reliable, efficient and can operate at higher power densities. With modern wide-bandgap (WBG) semiconductors, heat fluxes up to 500 W/cm2 are common. Using conventional cooling solutions such as pin-fins and microchannel heat sinks, it's becoming increasingly difficult to manage the high heat loads of the WBG semiconductors and it is not possible to maintain uniform cooling of each semiconductor. A need for an alternative cooling solution that can maintain WBG devices within their optimal temperature range and ensure cooling uniformity is highly required. Jet impingement for power electronics cooling has shown to be an effective approach where an array of liquid jets impinges on to a heated surface, which is commonly referred to as the baseplate. A modification to jet impingement, illustrated in Fig. 1 is studied in this work where the array of liquid jets impinges a ribbed baseplate to enhance convective heat transfer. The use of a ribbed baseplate and smooth baseplate is directly compared, with the trade-off between heat transfer enhancement and pressure drop being used to assess each cooling solution. A 60-40% (by volume) mixture of ethylene glycol-water is used as the coolant and the jet Reynolds number is varied from 3,000 to 11,000. An in-line array with four conical nozzles with exit diameter (d) is used to generate the jet array. In the jet array, the spacing (s) between each nozzle is 18.5d and the distance from the nozzle to baseplate (h) is 5d. The rib thickness (t), width (w) and spacing between each rib (l) is 0.25d. Both cooling solutions are investigated numerically. A RANS modelling approach is implemented and the k-ω SST turbulence model is used to model the turbulent nature of the flow. It was found that the use of ribs provided an enhanced heat transfer as indicated by a 30% increase in the average Nusselt number at the cost of a 5% increase in pressure drop. Enhanced heat transfer with the ribbed baseplate is contributed to increased surface area for convective cooling and increased turbulence near the baseplate. The ribbed and smooth baseplate provided good temperature uniformity with less than a 1% difference in the area averaged Nusselt numbers averaged over each heater area.

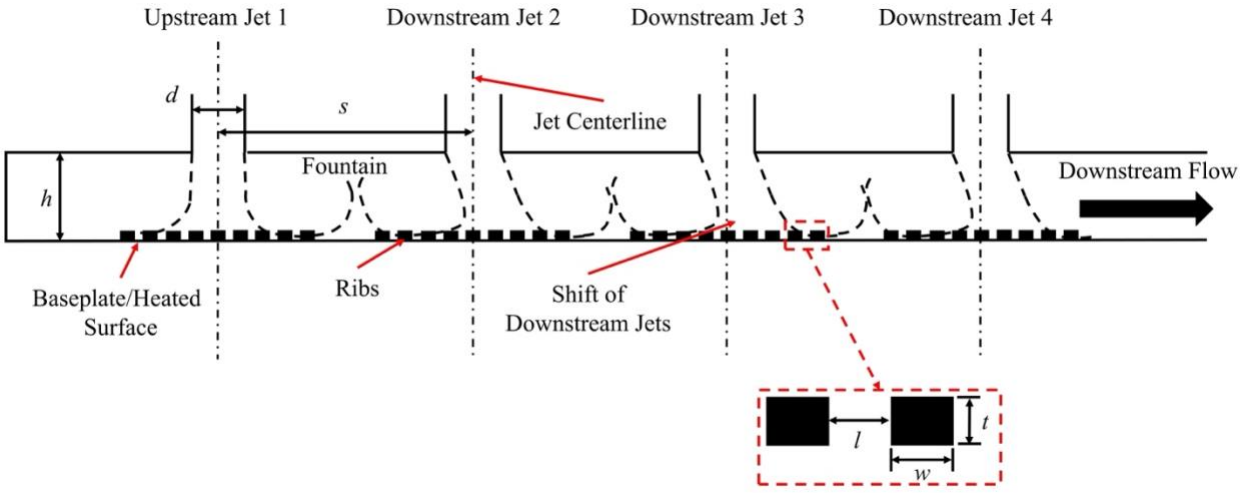

Study of Self-Oscillating Jets for the Cooling of Electronic Chips

Maziar Mosavati, Ronald Barron, Ram Balachandar

In the current study, an assessment of self-oscillating jets for use in cooling applications is investigated. Self-oscillating jets are a type of fluid jet where the flow oscillates without any external devices driving the oscillation. Jets emanating into a confined cavity exhibit self-oscillating behavior due to the Coanda effect. In the present study, the jet exits into a narrow rectangular cavity from a square nozzle at a Reynolds number of 54,000 based on average jet exit velocity and nozzle hydraulic diameter The heated devices, such as electronic chips, are located externally on the surface of the cavity, as shown in Fig. 1a. The three-dimensional unsteady Reynolds-Averaged Navier-Stokes (URANS) and energy equations are solved numerically to assess the thermal features of the flow field. The unsteady Elliptic Blending Reynolds Stress Model was used to model turbulence. The computational domain was discretized using a hexahedral mesh with 7 million cells. The governing flow equations were discretized using the finite volume method and solved using the commercial software STAR-CCM+. The time step was set at 0.01 ms, which produced a Courant number less than one. The fluid is water with a dynamic viscosity of 9.7x10-4 kg/(m.s), and the hot block heat flux is 105 W/m2 on each heated element. The present study is novel in the sense that it uses the jet(s) contained within the module to self-oscillate and provide for a more uniform cooling through a sweeping motion. The current study helps to identify regions with potentially higher heat transfer rates and greater surface temperature uniformity due to higher jet spread. To this end, the cooling effectiveness of two different arrangements of four heated devices is evaluated. The results demonstrate that the oscillatory flow field contributes to mixing and entrainment of flow in a cavity which is used for cooling applications. The self-oscillating jet increases heat transfer on a wider surface especially when the hot devices are located in a horizontal arrangement (Fig. 1b) compared to the vertical arrangement. The results shown in Fig. 1c demonstrate that the instantaneous surface-averaged Nusselt number of the self-oscillating jet varies periodically with time and a maximum peak of Nuav for the second hot block corresponds to a minimum value for the Nuav for the third hot block. Moreover, the shape of the instantaneous signals is symmetrical due to the sweeping motion of the jet.

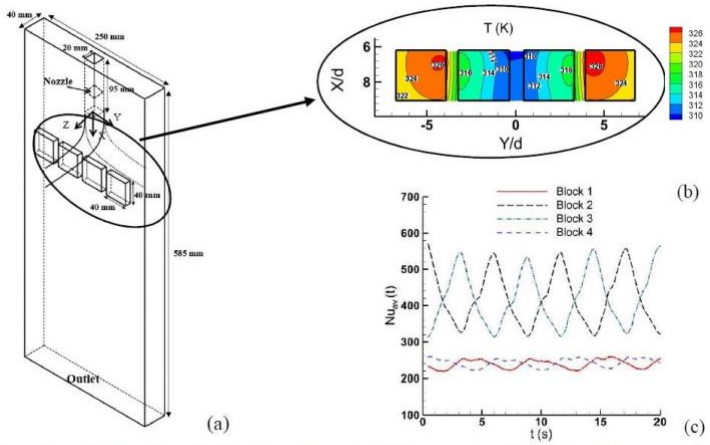

Fig. 1. Illustration of (a) a self-oscillating jet configuration, (b) temperature field (c) surface-averaged Nusselt number for a horizontal arrangement of hot blocks